Identification of ATP6V0A4 as a potential biomarker in renal cell carcinoma using integrated bioinformatics analysis

JINMING XU[1,2*], JIAHAO JIANG[3*], CONG YIN[1], YAN WANG[4] and BENTAO SHI[1]

[1]Department of Urology, Shenzhen Second People's Hospital/First Affiliated Hospital of Shenzhen University, Shenzhen, Guangdong 518035; [2]Department of Urology, Shantou University Medical College, Shantou, Guangdong 515041; [3]Department of Urology, Shenzhen Second People's Hospital, Clinical College of Anhui Medical University, Shenzhen, Guangdong 518035; [4]Department of Urology, Peking University Shenzhen Hospital, Shenzhen, Guangdong 518036, P.R. China

Abstract. Clear cell renal cell carcinoma (ccRCC) is the most common pathological type of renal cancer, and is associated with a high mortality rate, which is related to high rates of tumor recurrence and metastasis. The aim of the present study was to identify reliable molecular biomarkers with high specificity and sensitivity for ccRCC. A total of eight ccRCC-related expression profiles were downloaded from Gene Expression Omnibus for integrated bioinformatics analysis to screen for significantly differentially expressed genes (DEGs). Reverse transcription-quantitative (RT-q)PCR, western blotting and immunohistochemistry staining assays were performed to evaluate the expression levels of candidate biomarkers in ccRCC tissues and cell lines. In total, 255 ccRCC specimens and 165 adjacent normal kidney specimens were analyzed, and 344 significant DEGs, consisting of 115 upregulated DEGs and 229 downregulated DEGs, were identified. The results of Gene Ontology analysis suggested a significant enrichment of DEGs in 'organic anion transport' and 'small molecule catabolic process' in biological processes, in 'apical plasma membrane' and 'apical part of the cell' in cell components, and in 'anion transmembrane transporter activity' and 'active transmembrane transporter activity' in molecular functions. Kyoto Encyclopedia of Genes and Genomes pathway enrichment analysis indicated that the DEGs were significantly enriched in the 'phagosome', the 'PPAR signaling pathway', 'complement and coagulation cascades', the 'HIF-1 signaling pathway' and 'carbon metabolism'. Next, 7 hub genes (SUCNR1, CXCR4, VCAN, CASR, ATP6V0A4, VEGFA and SERPINE1) were identified and validated using The Cancer Genome Atlas database. Survival analysis showed that low expression of ATP6V0A4 was associated with a poor prognosis in patients with ccRCC. Additionally, received operating characteristic curves indicated that ATP6V0A4 could distinguish ccRCC samples from normal kidney samples. Furthermore, RT-qPCR, western blotting and immunohistochemistry staining results showed that ATP6V0A4 was significantly downregulated in ccRCC tissues and cell lines. In conclusion, ATP6V0A4 may be involved in tumor progression and regarded as a potential therapeutic target for the recurrence and metastasis of ccRCC.

Introduction

Renal cell carcinoma (RCC) is one of the most common malignancies of the urogenital system. In 2019, ~73,820 new cases and 14,770 deaths in the United States were due to RCC (1-3). The occurrence of RCC has been increasing at a rate of 2-4% per year (4). Based on the histological phenotype, RCC is categorized into four subcategories: Chromophobe, clear cell, collecting duct and papillary, with clear cell RCC (ccRCC) accounting for 80-90% of all RCC tumors (5). Attributable to the paucity of apparent early symptoms, 30% of patients are diagnosed with advanced-stage RCC in the first instance, leading to distant metastasis of tumor cells to the bones, the lungs, the brain and other important organs (6-9). Unfortunately, patients with metastatic ccRCC are insensitive to chemoradiotherapy (10), and the 5-year survival rate is only 8% (11). Although targeted therapy has been developed and approved for the treatment of ccRCC, patient outcomes

have not been notably improved due to extensive intertumoral heterogeneity (12). Thus, given the high incidence and mortality of ccRCC, it is necessary to identify novel molecular biomarkers for early detection and for improving prognosis.

Vacuolar H^+-ATPases (V-ATPases) participate in the regulation of intracellular and extracellular pH since they are a family of ATP-dependent proton pumps that acidify various intracellular organelles and extracellular environments; they play a vital role in several biological processes, such as membrane transport, protein processing and degradation, small molecule coupling transport, and other physiological processes, including urinary acidification and bone reabsorption (13). V-ATPases are composed of different subunits, which are divided into two main regions: A cytoplasmic domain, V1, for ATP hydrolysis, and a membrane domain, V0, which facilitates proton transport (14). The V0 domain subunit has four distinct subtypes a1-a4, which regulate the targeting of V-ATPases to different cellular membranes (15-17). ATP6V0A4 gene encoding a4 subunit, primarily expressed in kidneys and the epididymis, allows localization of V-ATPases to the plasma membrane of renal α-intercalated cells where it secretes H^+ into the urine (18).

Previous research showed high expression of ATP6V0A4 in breast cancer tissues, and knockdown of ATP6V0A4 using siRNA in the highly invasive MDA-MB-231 human breast cancer cell, suppressed invasiveness *in vitro* (18). Additionally, treatment of MDA-MB-231 cells with specific V-ATPase inhibitors, such as bafilomycin or concanamycin, exhibited a promising inhibitory effect on invasion (19). Moreover, knockdown of V-ATPases expression using siRNA in HCCLM3 cells (a human hepatocellular carcinoma cell line with high metastatic potential) effectively inhibited tumor growth and metastasis by reducing proton secretion and downregulating matrix metalloproteinase-2 and gelatinase activities (20). However, there are few studies on the differential expression, development and molecular mechanism of ATP6V0A4 in malignant tumors (14,21).

In the present study, given that ATP6V0A4 was specifically expressed in the kidney and epididymis, the correlation between ATP6V0A4 expression and clinicopathological characteristics of patients with ccRCC, as well as prognosis, was examined to ascertain the potential role of ATP6V0A4 as a candidate biomarker in the occurrence and progression of ccRCC.

Materials and methods

Dataset analysis. In the present study, eight ccRCC-related gene microarrays (GSE76351, GES6344, GSE15641, GSE16449, GSE47032, GSE66270, GSE53000 and GSE53757) (22-29) were acquired from the Gene Expression Omnibus (GEO) database (https://www.ncbi.nlm.nih.gov/geo/). The inclusion criteria were: i) ccRCC datasets; ii) specimens consisting of tumor and adjacent normal kidney tissues; iii) expression profiling assessed by microarray analysis; and iv) profiling data collected from human samples. In total, 255 ccRCC specimens and 165 adjacent normal kidney specimens were analyzed.

Identification of differentially expressed genes (DEGs). The limma package (30) in R version 4.0 (31) was used to compare

gene expression profiles between ccRCC tissues and the adjacent normal kidney tissues in the GEO datasets. The cut-off criterion for identifying DEGs was: |log$_2$ fold-change (FC)|>2. P<0.05 was considered to indicate a statistically significant difference.

Robust Rank Aggregation (RRA) method. Robust DEGs were identified using the core algorithm of the RRA R package (32), which was ranked consistently better than anticipated. This algorithm was parameter-free and was less affected by outliers, noise and errors. The screening criterion of |log$_2$ FC|>2 and an adjusted P-value of <0.05 was considered to indicate a statistically robust DEG.

Functional enrichment analyses. DEG analysis using Gene Ontology (GO) and Kyoto Encyclopedia of Genes and Genomes (KEGG) pathway enrichment analyses were conducted using DAVID (version 6.8) (33,34), and their potential functional relevance was explored. Biological processes (BPs), molecular functions (MFs) and cell components (CCs) were assessed by GO enrichment analysis, while pathway enrichment analysis was performed using KEGG. An adjusted P-value of <0.05 was considered to indicate a statistically significant difference.

Protein-protein interaction (PPI) network analysis. The PPI network of DEGs was established using STRING (http://string-db.org) (35). The parameter of interactive relationships among DEGs was set as highest confidence >0.9. Cytoscape (version 3.7.1) software (36) was used to visualize and analyze the network.

Hub gene selection and analysis. Identification of hub genes based on these DEGs was conducted using the cytoHubba (37) plug-in in Cytoscape, which provides 12 computed methods to analyze results. Hub genes were obtained by the intersection of the top 50 genes evaluated using the 12 methods. The receiver operating characteristic (ROC) curves were comprehensive indexes, which were utilized to reflect the sensitivity and specificity of hub genes and evaluate the potential value of hub genes as biomarkers in distinguishing the ccRCC tissues from adjacent normal kidney tissues.

The Cancer Genome Atlas (TCGA) database validation. TCGA (http://ualcan.path.uab.edu) was used to obtain information relating to the differential expression of hub genes in ccRCC and normal kidney tissues and determine the associations of the expression levels of these genes with prognosis. We chose the hub gene that was most significantly associated with survival for further analysis. The gene expression profiles were downloaded from TCGA (xenabrowser.net) to analyze the association between the hub gene and clinicopathological characteristics of patients with ccRCC.

Cell culture and ccRCC tissue specimens. In total, four ccRCC cell lines (ACHN, Caki-1, 786-O and 769-P), a papillary RCC cell line (Caki-2) and a human proximal tubular epithelial cell line (HK-2) were acquired from the American Type Culture Collection. All cell lines were cultured in DMEM, 1640 or McCoy's 5A (Gibco; Thermo Fisher Scientific, Inc.) supplemented with 10% FBS and 100 U/ml penicillin/streptomycin

in a humidified incubator supplied with 5% CO_2 air at 37˚C. In addition, a total of 23 pairs of ccRCC tissues and adjacent normal kidney tissues were collected from ccRCC patients [including 12 males and 11 females, and the median age was 58 (43-78) years] who had not received chemoradiotherapy. Patients were diagnosed at the Department of Urology, Peking University Shenzhen Hospital (Shenzhen, China) between March 2020 and March 2021. All experiments strictly followed the Declaration of Helsinki and ethical approval was obtained from Peking University Shenzhen Hospital Ethics Committee (approval no. 20090017). All patients were informed of the intent to collect their specimen, the potential risks and the purposes of the study, and they provided written informed consent.

Reverse transcription-quantitative (RT-q)PCR. Total RNA from cell lines and tissue was extracted using TRIzol® reagent (Takara Bio, Inc.), and 1 μg total RNA was reverse transcribed using a PrimeScript™ RT reagent Kit with gDNA Eraser according to the manufacturer's protocol (Takara Bio, Inc.). Next, qPCR was performed on a LightCycler 480 (Roche Diagnostics) using a SYBR Premix Ex Taq™ II Kit (Takara Bio, Inc.). Thermocycling conditions were as follows: Initial denaturation at 95˚C for 30 sec, followed by 40 cycles of 95˚C for 5 sec, 60˚C for 30 sec and 72˚C for 30 sec, then final extension at 95˚C for 1 sec, 65˚C for 1 min and 95˚C for 15 sec. The primers used in this study were synthesized by Sangon Biotech, Co., Ltd., with the following sequences: GAPDH forward, 5'-CCACTCCTCCACCTTTGACG-3' and reverse, 5'-CTGGTGGTCCAGGGGTCTTA-3'; ATP6V0A4 forward, 5'-CTGCCGAGGAAACGTGTACTT-3' and reverse, 5'-GGC TCGAAACCCATCACAGA-3'; SUCNR1 forward, 5'-TGC TGGCAGAGTTCCTGTCAAG-3' and reverse, 5'-AGTTGC ATTCCATGCCATGATCC-3'; and SERPINE1 forward, 5'-AGAGCGCTGTCAAGAAGACC-3' and reverse, 5'-AGT TCTCAGAGGTGCCTTGC-3'. The expression of hub genes was normalized to the respective GAPDH expression and calculated by the $2^{-\Delta\Delta Cq}$ method (38).

Western blotting. Protein samples from cells were collected using RIPA lysis buffer and protease inhibitor (Beyotime Institute of Biotechnology). Protein concentrations were determined using a BCA protein assay kit (Takara Bio, Inc.). A total of 20 μg protein/lane was loaded on 10% SDS-gels, resolved using SDS-PAGE and transferred to PVDF membranes, and then the membranes were blocked using 5% skimmed milk for 2 h at room temperature. Subsequently, the membranes were incubated with the primary antibodies overnight at 4˚C, followed by subsequent incubation with the relevant secondary antibody for 1 h at room temperature. The primary antibodies used were an anti-ATP6V0A4 antibody (1:3,000; cat. no. ab97440; Abcam) and an anti-GAPDH antibody (1:10,000; cat. no. AC002; ABclonal Biotech Co., Ltd.). The secondary antibodies used were an anti-rabbit (1:2,000; cat. no. 7074; Cell Signaling Technology, Inc.) and an anti-mouse IgG HRP-linked antibody (1:2,000; cat. no. 7076; Cell Signaling Technology, Inc.). Signals were visualized using a chemiluminescence imaging system (Tanon-5200Multi; Tanon Science and Technology Co., Ltd.) and BeyoECL Star reagent (Beyotime Institute of Biotechnology). ImageJ v1.53 (National Institutes of Health) was used for densitometry.

Immunohistochemistry staining. Single spot tissue microarray (TMA) slides (30 points of ccRCC, 30 points of adjacent normal kidney tissues; cat. no. HKid-CRC060CS-01, Shanghai Outdo Biotech Company) were prepared and incubated with the ATP6V0A4 rabbit antibody (1:500; cat. no. 21570-1-AP; ProteinTech Group, Inc.) at 4˚C overnight. And the rabbit streptavidin-biotin detection system (OriGene Technologies, Inc.) was used for staining. Two experienced pathologists evaluated the results according to the staining intensity [0 (negative), 0.5+, 1+, 2+ and 3+] and the positive staining rate (0-100%). Next, the total score (0-300%) was calculated as the product of the staining intensity score and positive staining rate score. Low expression was defined as expression less than or equal to the median score (0%), whereas a score greater than the median was classed as high expression.

Statistical analysis. The expression of ATP6V0A4 between ccRCC tissues and adjacent normal kidney tissues was analyzed using Fisher's exact test. The association between ATP6V0A4 and each clinicopathological variable was analyzed using a χ^2 test. Data are presented as the mean ± SD of at least three repeats. Unpaired student's t-test was used for comparing expression levels of hub genes between ccRCC tissues and adjacent normal kidney tissues. Survival curves were analyzed using the Kaplan-Meier method for patients with high or low expression levels of hub genes and were evaluated for statistical significance using the log-rank test. One-way ANOVA followed by Dunnett's post-hoc test was utilized for comparing the expression of ATP6V0A4 among ccRCC cell lines. GraphPad Prism version 7 (GraphPad Software, Inc.) was used for all statistical analyses. $P<0.05$ was considered to indicate a statistically significant difference.

Results

Identification of DEGs in each GEO dataset. Integrated bioinformatics analyses were used to screen for the significant DEGs in the ccRCC datasets (Fig. 1). First, the core phrase 'clear cell renal cell carcinoma' was searched in the GEO database, and the GSE76351, GES6344, GSE15641, GSE16449, GSE47032, GSE66270, GSE53000 and GSE53757 microarray datasets were downloaded. In total, 255 cases of ccRCC specimens and 165 cases of adjacent normal kidney specimens were analyzed. DEGs in each GEO dataset were identified based on the cut-off criteria. Amongst all the DEGs in each dataset, there were 247 upregulated and 284 downregulated genes (GES6344), 88 upregulated and 179 downregulated genes (GSE15641), 183 upregulated and 428 downregulated genes (GSE16449), 185 upregulated and 337 downregulated genes (GSE47032), 58 upregulated and 201 downregulated genes (GSE53000), 365 upregulated and 521 downregulated genes (GSE53757), 718 upregulated and 591 downregulated genes (GSE66270), and 252 upregulated and 471 downregulated genes (GSE76351). Each of these was plotted as volcano plots (Fig. 2A-H).

Selection of robust DEGs using the RRA method. The core algorithm of RRA was utilized to identify robust DEGs in the different datasets. A total of 344 significantly robust DEGs, consisting of 115 upregulated DEGs and 229 downregulated DEGs, were identified in the eight GEO datasets. The top 20 DEGs are presented using a heatmap (Fig. 2I).
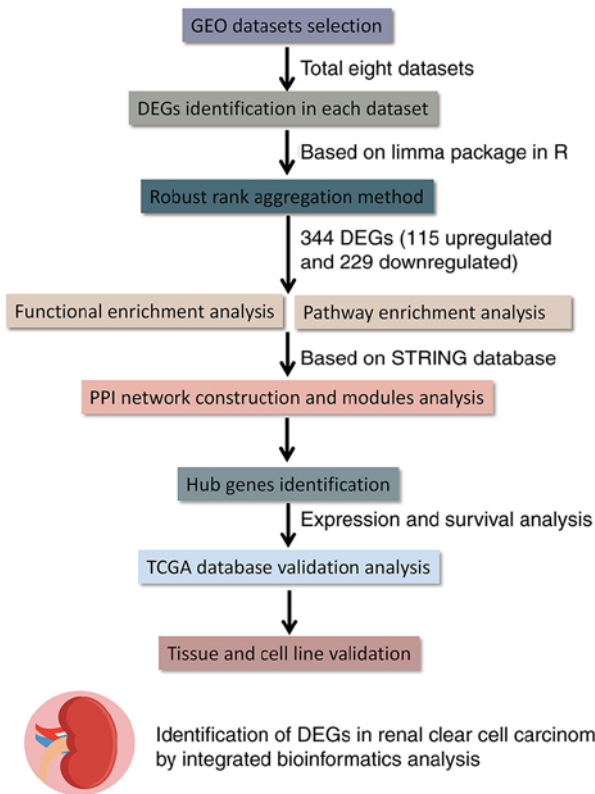
Figure 1. Workflow of the present study. GEO, Gene Expression Omnibus; DEG, Differentially Expressed Gene; PPI, Protein-Protein Interaction; TCGA, The Cancer Genome Atlas.

Functional and pathway enrichment analyses. GO and KEGG pathway enrichment analyses were used to evaluate the biological functions of the significant DEGs. The GO results suggested a significant enrichment of DEGs in 'organic anion transport' and 'small molecule catabolic process' in BPs, in 'apical plasma membrane' and 'apical part of the cell' in CCs, and in 'anion transmembrane transporter activity' and 'active transmembrane transporter activity' in MFs (Fig. 3A). The KEGG pathway enrichment analysis indicated that DEGs were significantly enriched in the 'phagosome', the 'PPAR signaling pathway', 'complement and coagulation cascades', the 'HIF-1 signaling pathway' and 'carbon metabolism' (Fig. 3B).

Construction of the PPI network and identification of hub genes. After introducing the significant DEGs into the STRING database, the interaction among DEGs was plotted as a PPI network. Based on the aforementioned results, 7 hub genes (SUCNR1, CXCR4, VCAN, CASR, ATP6V0A4, VEGFA and SERPINE1) were identified based on the intersection of the top 50 genes (Fig. 4A). Cytoscape was utilized for further visualizing the network of hub genes (Fig. 4B). ROC curves based on data obtained from TCGA were plotted to evaluate the diagnostic values of the hub genes. The area under the curve values of SERPINE1, CXCR4, VEGFA, VCAN, ATP6V0A4, SUCNR1 and CASR were 0.7907, 0.9745, 0.9624, 0.8137, 0.9545, 0.8514, and 0.9829, respectively ($P<0.0001$; Fig. 4C-I).

Validation and survival analysis based on TCGA. To verify the differential expression of hub genes, the corresponding gene expression profiles of kidney renal clear cell carcinoma (KIRC) were downloaded from TCGA. As shown in Fig. 5A, all hub genes were significantly differentially expressed. Combined with the survival analysis, it was found that ATP6V0A4, SUCNR1, CASR, CXCR4, and SERPINE1 were significantly associated with prognosis (Fig. 5B). Since CASR and CXCR4 have been studied in ccRCC (39,40), the remaining three genes were selected for further validation.

Validation of hub genes by RT-qPCR. The expression levels of three hub genes (ATP6V0A4, SUCNR1 and SERPINE1) were examined by RT-qPCR in 23 pairs of ccRCC tissues and adjacent normal tissues. The results indicated that the expression levels of ATP6V0A4 ($P=0.0007$) and SUCNR1 ($P<0.0001$) in ccRCC tissues were significantly lower than those in the adjacent normal kidney tissues (Fig. 6A-D), while the expression of SERPINE1 did not differ significantly between the cancerous and paracancerous tissues (Fig. 6E and F). Since the difference in expression of ATP6V0A4 between the cancerous and paracancerous tissues was greater than that of SUCNR1 and ATP6V0A4 was specifically expressed in the kidney, a focus was placed on the role of ATP6V0A4 in ccRCC progression.

ATP6V0A4 expression is downregulated in ccRCC. The difference in the expression profiles of ATP6V0A4 between ccRCC tissues and the adjacent normal kidney tissues in eight GEO datasets (GSE76351, GES6344, GSE15641, GSE16449, GSE47032, GSE66270, GSE53000 and GSE53757) was analyzed. The results showed significantly lower expression of ATP6V0A4 in ccRCC tissues compared with that in the adjacent normal kidney tissues (all $P<0.0001$) (Fig. 7A). These results were also confirmed by immunohistochemistry. There was a significant downregulation of the ATP6V0A4 protein expression levels in the ccRCC tissues compared with that in the adjacent normal kidney tissues ($P<0.001$; Fig. 7B; Table I). In addition, how ATP6V0A4 expression was associated with the clinicopathological characteristics was determined based on data from 534 patients with ccRCC obtained from TCGA. It was shown that dysregulated expression of ATP6V0A4 in ccRCC was associated with the 5-year survival rate, but not with age, sex, primary tumor (T stage), lymph node involvement (N stage), distant metastasis (M stage) and AJCC stage of patients with ccRCC (Table II). Combined with previous Kaplan-Meier survival analysis, it was shown that patients with ccRCC and high ATP6V0A4 expression had a better prognosis.

For further study, both RT-qPCR and western blotting experiments were conducted to explore the expression level of ATP6V0A4 in RCC cell lines. The results showed that ATP6V0A4 was significantly downregulated in 769-P, ACHN, and Caki-2 cell lines compared with that in HK-2 cells at the transcription level (Fig. 7C). While ATP6V0A4 level was remarkably decreased in all 5 RCC cell lines compared with that in HK-2 cells at translational level (Fig. 7D).

Discussion

As the most common subtype of RCC, ccRCC has an increasing prevalence, and is associated with a poor prognosis and considerable metastatic potential (41,42). Despite the several advances in establishing prediction models based on
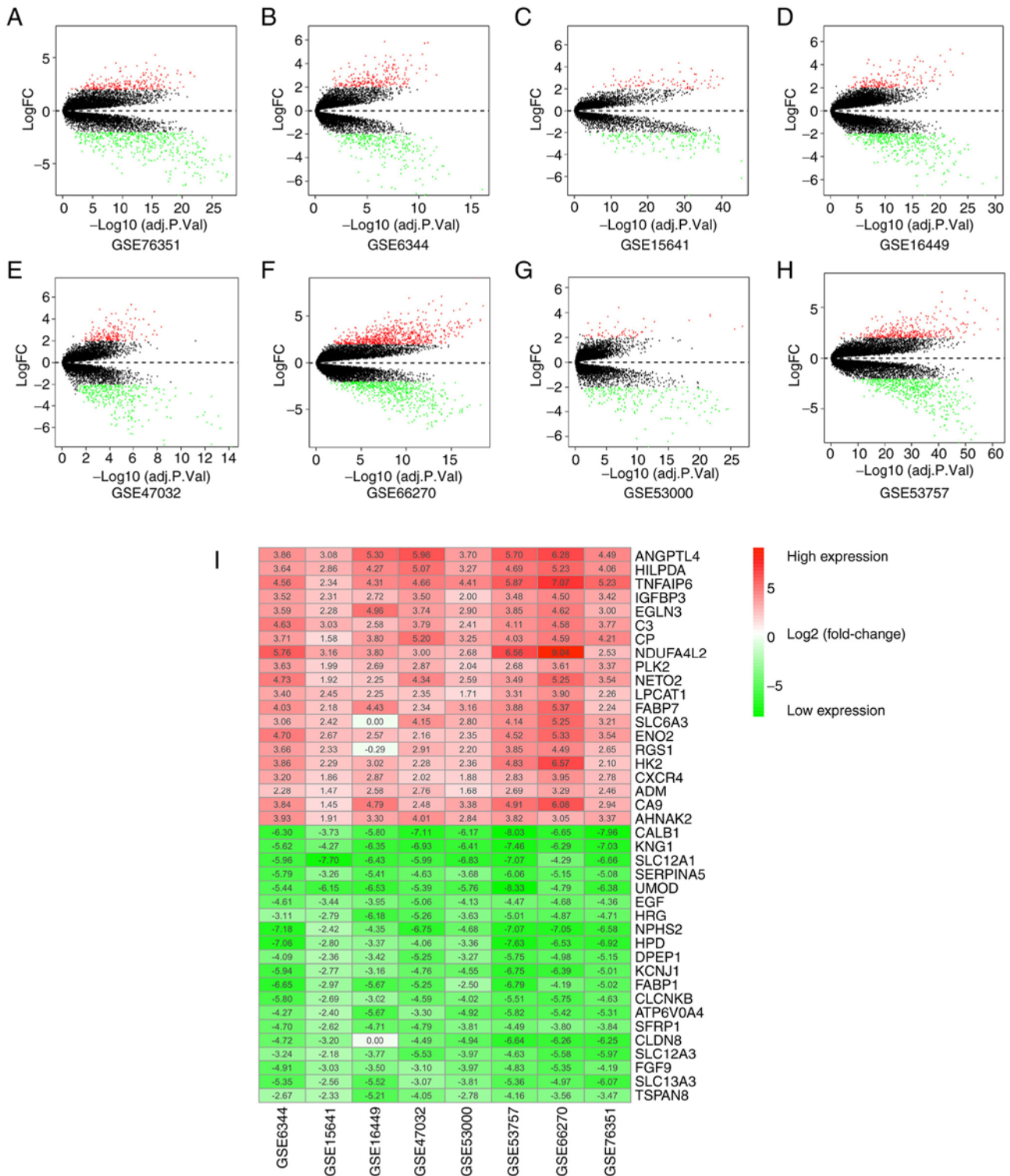
Figure 2. Identification of DEGs between clear cell renal cell carcinoma tissues and normal tissues in each Gene Expression Omnibus dataset. (A-H) Volcano plots of the distribution of DEGs in each dataset. (I) Heatmaps of the expression of the top 20 upregulated and downregulated DEGs using the Robust Rank Aggregation method. DEG, differentially expressed gene.

the clinical characteristics of ccRCC, exploration of the molecular mechanisms of tumorigenesis, increased understanding of the development and metastasis of ccRCC, and the countless targeted and immunosuppressive therapeutics, the strategies for curing ccRCC remain limited (43-45). Additionally, the generation of drug resistance remains a thorny issue during treatment. Consequently, there is an urgent need to identify

highly specific and sensitive candidate biomarkers, elucidate the molecular mechanisms underlying tumorigenesis and metastasis, and develop novel and effective treatment regimens for patients with ccRCC.

Bioinformatics is a transdisciplinary research approach, specifically used to screen out DEGs to understand the molecular and genetic basis of diseases. In the present study, eight GEO
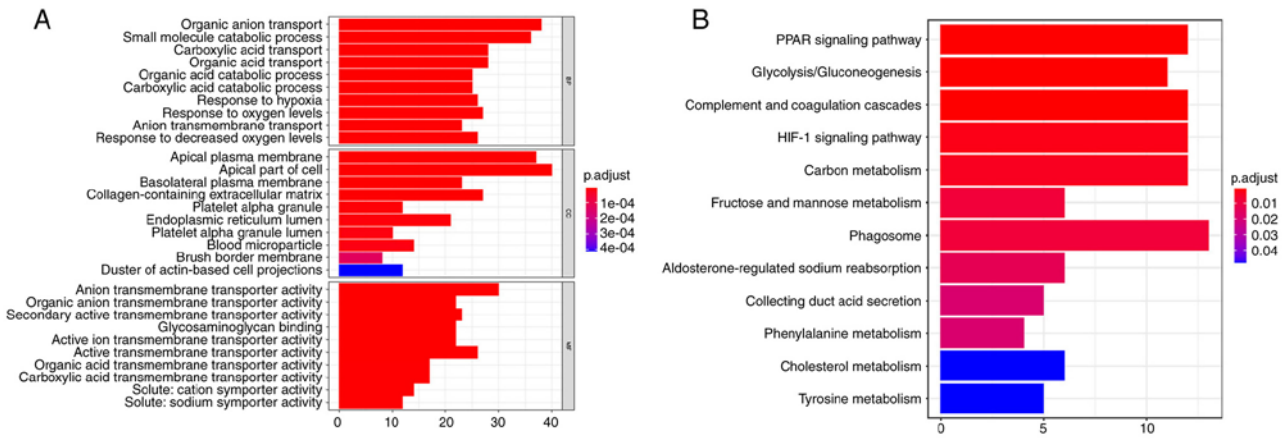
Figure 3. Functional characteristic analysis of the DEGs. (A) GO enrichment analysis of the significant DEGs. (B) KEGG pathway enrichment analysis of significant DEGs. DEG, differentially expressed gene; GO, Gene Ontology; KEGG, Kyoto Encyclopedia of Genes and Genomes.
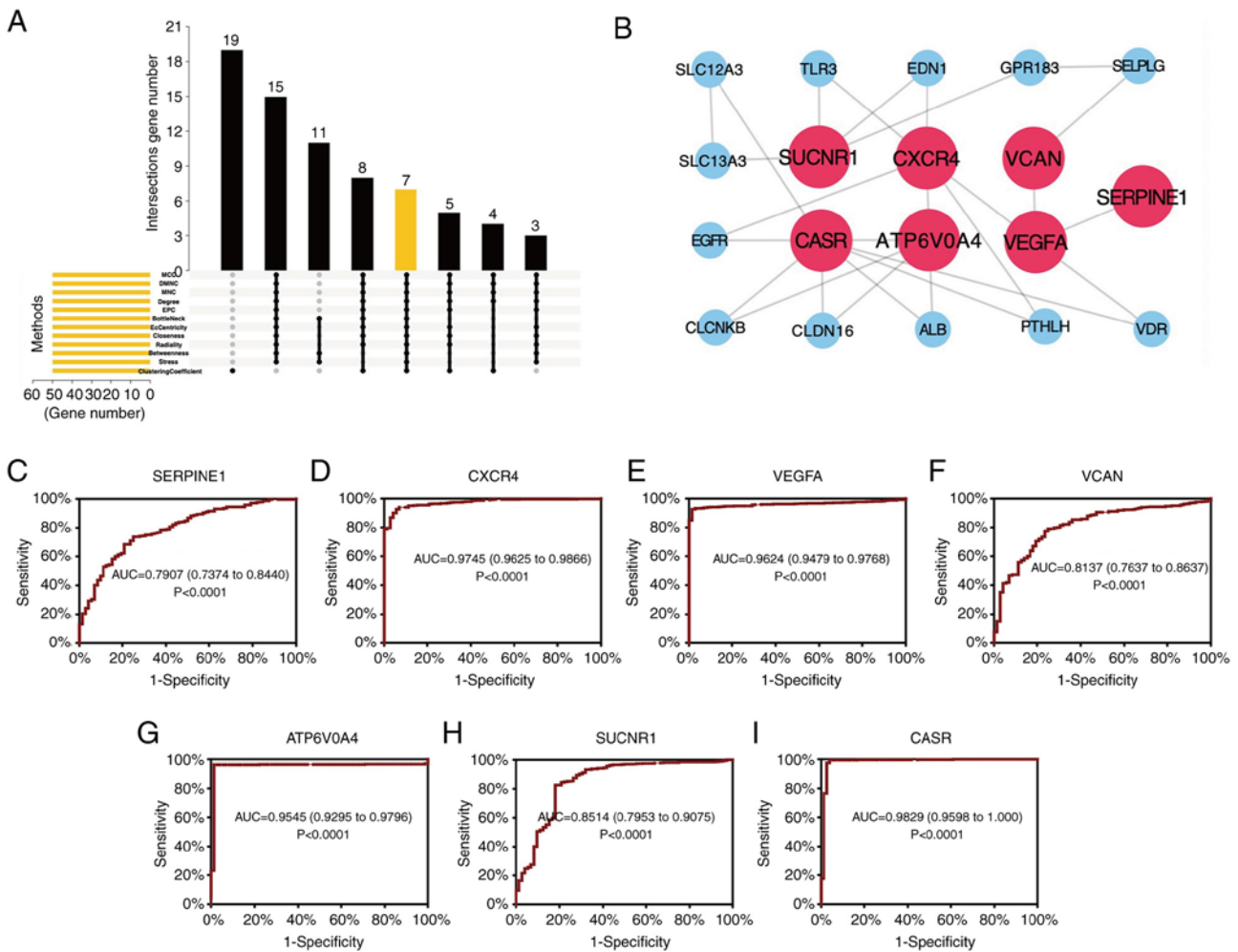

Figure 4. Construction of the PPI network and identification of hub genes. (A) Intersectional plot of the top 50 genes evaluated using 12 methods in the 8 datasets. (B) PPI network of the hub genes. (C-I) Receiver operating characteristic curves of the hub genes, (C) SERPINE1, (D) CXCR4, (E) VEGFA, (F) VCAN, (G) ATP6V0A4, (H) SUCNR1 and (I) CASR. AUC, area under the curve; MNC, Maximum Neighborhood Component; DMNC, Density of Maximum Neighborhood Component; MCC, Maximal Clique Centrality; EPC, Edge Percolated Component.

datasets were analyzed using bioinformatics analysis. A total of 344 significantly robust DEGs, including 115 upregulated and 229 downregulated, were identified using the RRA method. Among them, 7 hub genes (SUCNR1, CXCR4, VCAN, CASR, ATP6V0A4, VEGFA and SERPINE1) were identified based on the intersection of the top 50 genes evaluated using cytoHubba. Furthermore, data obtained from TCGA was combined with the clinical specimens to evaluate the expression of ATP6V0A4

Table I. Expression of ATP6V0A4 in the cancerous and paracancerous tissues.

| Tissue sample | No. of cases | ATP6V0A4 expression | | P-value |
		High	Low	
ccRCC tissues	30	1	29	<0.001
Adjacent tissues	29	29	0	

Table II. Association between ATP6V0A4 expression and clinicopathological characteristics of patients with clear cell renal cell carcinoma based on data obtained from The Cancer Genome Atlas.8800240497.

| Clinicopathological variable | ATP6V0A4 expression | | χ^2 value | P-value |
	Low, n (%)	High, n (%)		
No. of cases	267	267	-	-
Sex			0.825	0.3637
Male	179 (67.0%)	169 (63.3%)		
Female	88 (33.0%)	98 (36.7%)		
Age, years			2.719	0.0991
<60	114 (42.7%)	133 (49.8%)		
≥60	153 (57.3%)	134 (50.2%)		
Pathological T stage			4.415	0.2200
T1	130 (48.7%)	144 (53.9%)		
T2	40 (15.0%)	30 (11.2%)		
T3	89 (33.3%)	88 (33.0%)		
T4	8 (3.0%)	3 (1.1%)		
Pathological N stage			4.124	0.1272
N0	122 (45.7%)	118 (44.2%)		
N1	4 (1.5%)	12 (4.5%)		
NX	141 (52.8%)	137 (51.3%)		
Pathological M stage			0.3309	0.8475
M0	212 (79.4%)	212 (79.4%)		
M1	37 (13.9%)	41 (15.4%)		
MX	16 (6.0%)	14 (5.2%)		
AJCC stage			2.333	0.5063
I	128 (47.9%)	140 (52.4%)		
II	34 (12.7%)	24 (9.0%)		
III	63 (23.6%)	60 (22.5%)		
IV	41 (15.4%)	41 (15.4%)		
Survival time, years			6.101	0.0135[a]
<5	204 (76.4%)	177 (66.3%)		
≥5	62 (23.2%)	87 (32.6%)		

Certain patients had incomplete data. [a]P<0.05. AJCC, American Joint Committee on Cancer.

in ccRCC and its association with clinicopathological factors and clinical outcomes. The data suggested that the expression of ATP6V0A4 was significantly downregulated in ccRCC, and significantly associated with age and survival. However, due to the deficiency of clinicopathological characteristics and follow-up information for the tissue samples, clinical correlation and survival analysis could not be performed.

Previous studies have reported that ATP6V0A4 is highly expressed in highly invasive breast cancer and glioma (14,18). However, in the present study, it was found that ATP6V0A4 expression was significantly downregulated in ccRCC tissues and that this downregulation was indicative of a poor prognosis. Similar results were also observed *in vitro* in ccRCC cell lines. Since proton pumps at the plasma membrane are
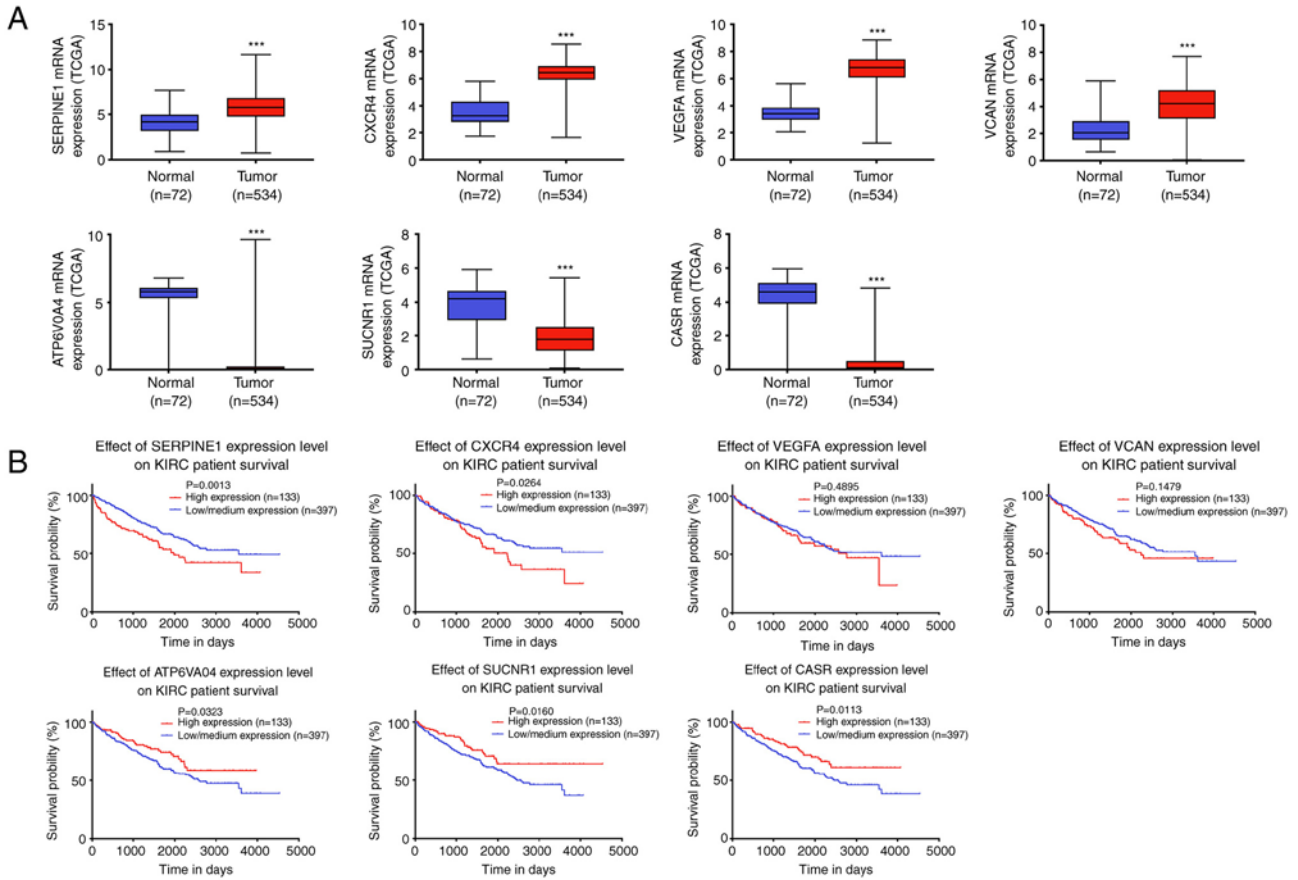
Figure 5. Validation and survival analysis based on data obtained from TCGA. (A) Box plots of expression levels of the hub genes in clear cell renal cell carcinoma and normal kidney tissue. ***P<0.001 vs. normal. (B) The corresponding Kaplan-Meier survival analyses. TCGA, The Cancer Genome Atlas; KIRC, Kidney renal clear cell carcinoma.
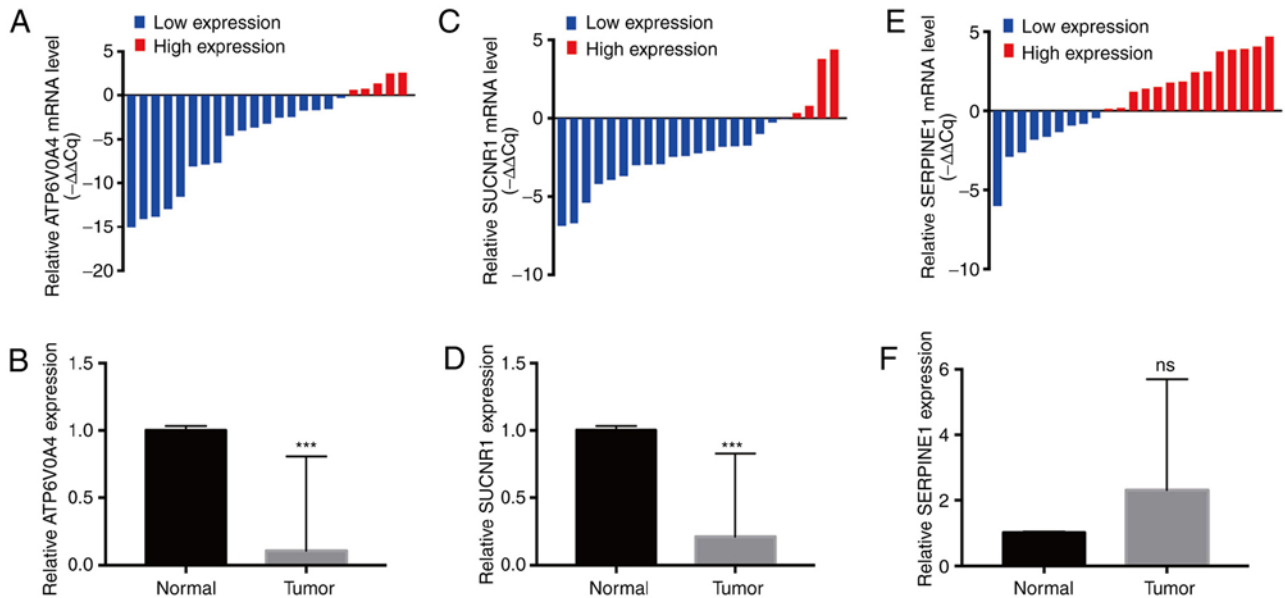

Figure 6. Validation of the expression of the differentially expressed hub genes using reverse transcription-quantitative PCR. (A and B) The expression of ATP6V0A4 was significantly downregulated in ccRCC tissues. (C and D) The expression of SUCNR1 was significantly downregulated in ccRCC tissues. (E and F) The expression of SERPINE1 did not differ between ccRCC tissues and paracancerous tissues. ccRCC, clear cell renal cell carcinoma; ***P<0.001 vs. normal; ns, not significant.

highly enriched in renal α-intercalated cells, ATP6V0A4 is tissue-restricted and replaces generic subunits of V-ATPases (46), which indicated that ATP6V0A4 was abundant in normal kidney tissues. Normal renal cells underwent
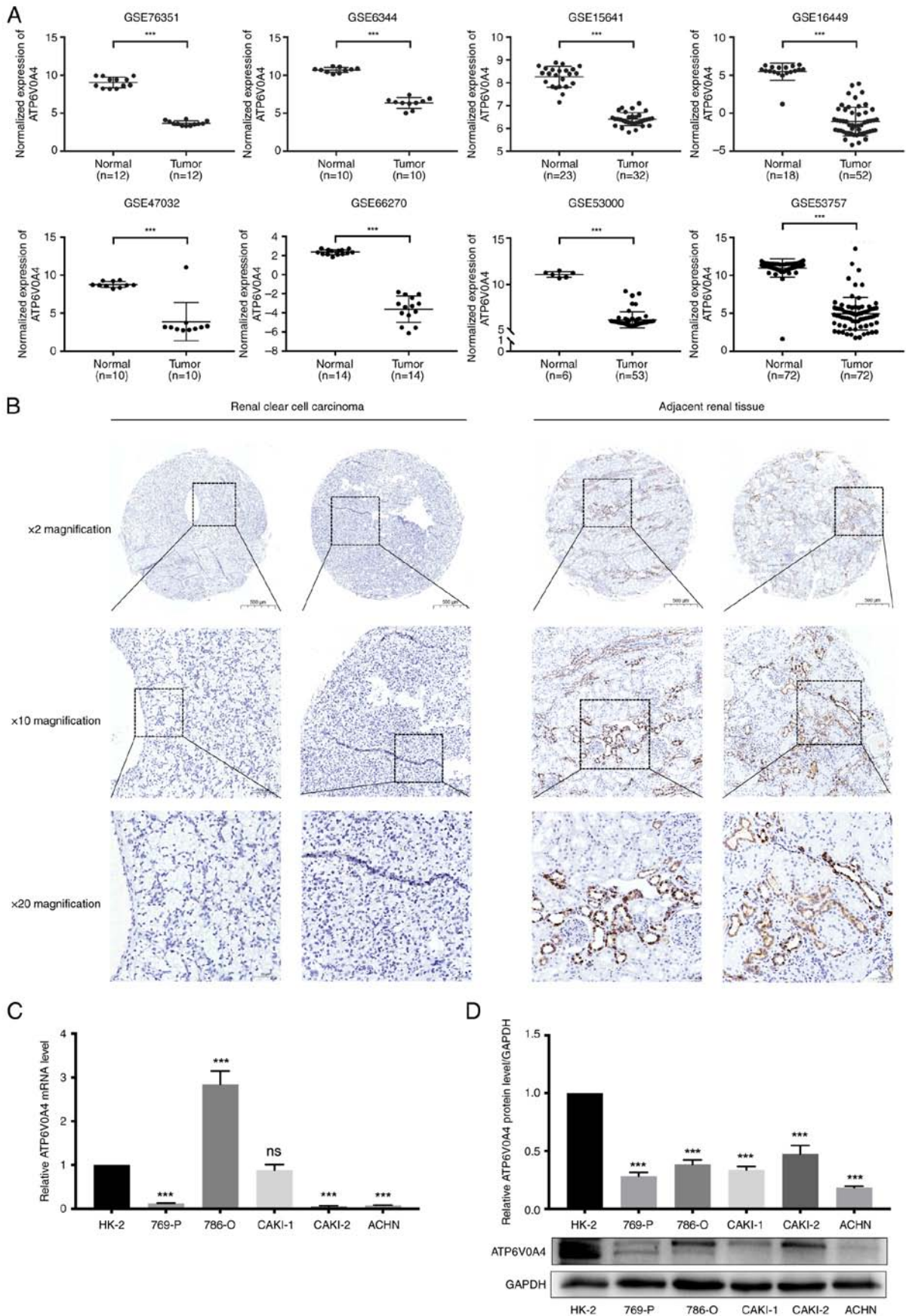
Figure 7. ATP6V0A4 is downregulated in ccRCC. (A) The expression of ATP6V0A4 in ccRCC tissues was significantly lower than that in adjacent renal tissues in eight Gene Expression Omnibus datasets (GSE76351, GES6344, GSE15641, GSE16449, GSE47032, GSE66270, GSE53000 and GSE53757). ***P<0.001 vs. normal. (B) The results of immunohistochemistry staining revealed that ATP6V0A4 protein expression was lower in ccRCC tissues than that in the adjacent renal tissues. (C) ATP6V0A4 was significantly downregulated in 769-P, ACHN and CAKI-2 cell lines compared with that in HK-2 cells at the transcription level. (D) Combined western blotting assay and densitometry indicated that ATP6V0A4 was remarkably decreased in all 5 RCC cell lines compared with that in HK-2 cells at the translational level. ccRCC, clear cell renal cell carcinoma; ***P<0.001 vs. HK-2; ns, not significant.

a neoplastic transformation and lost the ability to differentiate and mature to varying degrees, which led to the loss of normal structure in the kidney and replacement by tumor cells. It was speculated that given the high enrichment of ATP6V0A4 in normal renal tissues, the decreased expression of ATP6V0A4 resulted in the loss of normal tissue structure in renal cancer.

As previously reported, the dysregulation of ATP6V0A4 plays a vital role in tumor progression. The knockdown of ATP6V0A4 has been shown to significantly inhibit cell invasion in breast cancer by decreasing the targeting of V-ATPases to the plasma membrane of MDA-MB-231 cells (18). The V-ATPases have since been found to be present at the plasma membranes of several invasive tumor cells, including melanoma, Ewing sarcoma, and liver, lung, ovarian, esophageal, prostate and pancreatic cancer (47-54). The V-ATPases are heavily involved in tumor cell hallmarks such as migration and invasion by activating secreted cathepsin through local acidification of the extracellular environment to degrade the basement membrane and extracellular matrix proteins or by activating other secreted proteases such as matrix metalloproteinases (55,56). Several studies have demonstrated that pharmacological inhibition of V-ATPases results in potent antitumor and anti-metastatic effects *in vitro* and *in vivo* (13,57-61). Treatment of highly invasive MDA-MB-231 and MCF10-CA1a human breast cancer cells with specific V-ATPase inhibitors such as concanamycin A and bafilomycin appreciably suppressed the invasive ability *in vitro* (19,62). Additionally, Kulshrestha *et al* (51) found that targeted inhibition of V-ATPase restrained ovarian tumor invasion via regulation of matrix metalloproteinase activity. Further research needs to evaluate the expression patterns of multiple subunits and determine whether the activity of V-ATPases can be regulated by changes in the expression of ATP6V0A4 in ccRCC.

In conclusion, the bioinformatics analyses performed in the present study showed that ATP6V0A4 gene expression was significantly different between renal cancer tissues and para-cancerous tissues. The upregulated expression of ATP6V0A4 was associated with the improved survival of patients with ccRCC, which may provide a basis for targeted drug therapy. Exploring the mechanisms underlying the effects of ATP6V0A4 in RCC may assist in identifying novel druggable targets to improve the management of patients with ccRCC.

Acknowledgements

Not applicable.

Funding

Availability of data and materials

The datasets used and/or analyzed during the present study are available from the corresponding author on reasonable request.

Authors' contributions

JX, JJ and CY performed the experiments and analyzed the data. JX, JJ and YW wrote the manuscript. JX, YW and BS designed the study. JX, JJ and BS confirm the authenticity of all the raw data. All authors have read and approved the final manuscript.

Ethics approval and consent to participate

Patients were diagnosed at the Department of Urology, Peking University Shenzhen Hospital, China. All experiments strictly adhered to the guidelines described in the Declaration of Helsinki, and ethical approval was obtained from the Ethics Committee of Peking University Shenzhen Hospital (approval no. 20090017). All patients were informed of the intent to collect their specimen, the potential risks and the purposes of the study, and they provided written informed consent.

Patient consent for publication

All patients provided consent for their information to be published.

Competing interests

The authors declare that they have no competing interests.

References

1. Xu WH, Xu Y, Wang J, Wan FN, Wang HK, Cao DL, Shi GH, Qu YY, Zhang HL and Ye DW: Prognostic value and immune infiltration of novel signatures in clear cell renal cell carcinoma microenvironment. Aging (Albany NY) 11: 6999-7020, 2019.
2. Bray F, Ferlay J, Soerjomataram I, Siegel RL, Torre LA and Jemal A: Global cancer statistics 2018: GLOBOCAN estimates of incidence and mortality worldwide for 36 cancers in 185 countries. CA Cancer J Clin 68: 394-424, 2018.
3. Siegel RL, Miller KD and Jemal A: Cancer statistics, 2017. CA Cancer J Clin 67: 7-30, 2017.
4. Butz H, Szabó PM, Nofech-Mozes R, Rotondo F, Kovacs K, Mirham L, Girgis H, Boles D, Patocs A and Yousef GM: Integrative bioinformatics analysis reveals new prognostic biomarkers of clear cell renal cell carcinoma. Clin Chem 60: 1314-1326, 2014.
5. Wang Q, Tang H, Luo X, Chen J, Zhang X, Li X, Li Y, Chen Y, Xu Y and Han S: Immune-associated gene signatures serve as a promising biomarker of immunotherapeutic prognosis for renal clear cell carcinoma. Front Immunol 13: 890150, 2022.
6. Sacco E, Pinto F, Sasso F, Racioppi M, Gulino G, Volpe A and Bassi P: Paraneoplastic syndromes in patients with urological malignancies. Urol Int 83: 1-11, 2009.
7. Flanigan RC, Campbell SC, Clark JI and Picken MM: Metastatic renal cell carcinoma. Curr Treat Options Oncol 4: 385-390, 2003.
8. Jonasch E, Walker CL and Rathmell WK: Clear cell renal cell carcinoma ontogeny and mechanisms of lethality. Nat Rev Nephrol 17: 245-261, 2021.
9. Ke J, Chen J and Liu X: Analyzing and validating the prognostic value and immune microenvironment of clear cell renal cell carcinoma. Anim Cells Syst (Seoul) 26: 52-61, 2022.
10. Lai Y, Tang F, Huang Y, He C, Chen C, Zhao J, Wu W and He Z: The tumour microenvironment and metabolism in renal cell carcinoma targeted or immune therapy. J Cell Physiol 236: 1616-1627, 2021.
11. Choueiri TK and Motzer RJ: Systemic therapy for metastatic renal-cell carcinoma. N Engl J Med 376: 354-366, 2017.
12. Li Z, Xu H, Yu L, Wang J, Meng Q, Mei H, Cai Z, Chen W and Huang W: Patient-derived renal cell carcinoma organoids for personalized cancer therapy. Clin Transl Med 12: e970, 2022.
13. Stransky L, Cotter K and Forgac M: The function of V-ATPases in cancer. Physiol Rev 96: 1071-1091, 2016.

14. Gleize V, Boisselier B, Marie Y, Poëa-Guyon S, Sanson M and Morel N: The renal v-ATPase a4 subunit is expressed in specific subtypes of human gliomas. Glia 60: 1004-1012, 2012.
15. Cotter K, Stransky L, McGuire C and Forgac M: Recent insights into the structure, regulation, and function of the V-ATPases. Trends Biochem Sci 40: 611-622, 2015.
16. Breton S and Brown D: Regulation of luminal acidification by the V-ATPase. Physiology (Bethesda) 28: 318-329, 2013.
17. Sun-Wada GH and Wada Y: Vacuolar-type proton pump ATPases: Acidification and pathological relationships. Histol Histopathol 28: 805-815, 2013.
18. Hinton A, Sennoune SR, Bond S, Fang M, Reuveni M, Sahagian GG, Jay D, Martinez-Zaguilan R and Forgac M: Function of a subunit isoforms of the V-ATPase in pH homeostasis and in vitro invasion of MDA-MB231 human breast cancer cells. J Biol Chem 284: 16400-16408, 2009.
19. Sennoune SR, Bakunts K, Martínez GM, Chua-Tuan JL, Kebir Y, Attaya MN and Martínez-Zaguilán R: Vacuolar H⁺-ATPase in human breast cancer cells with distinct metastatic potential: Distribution and functional activity. Am J Physiol Cell Physiol 286: C1443-C1452, 2004.
20. Lu X, Qin W, Li J, Tan N, Pan D, Zhang H, Xie L, Yao G, Shu H, Yao M, et al: The growth and metastasis of human hepatocellular carcinoma xenografts are inhibited by small interfering RNA targeting to the subunit ATP6L of proton pump. Cancer Res 65: 6843-6849, 2005.
21. Su K, Collins MP, McGuire CM, Alshagawi MA, Alamoudi MK, Li Z and Forgac M: Isoform a4 of the vacuolar ATPase a subunit promotes 4T1-12B breast cancer cell-dependent tumor growth and metastasis in vivo. J Biol Chem 298: 102395, 2022.
22. Gumz ML, Zou H, Kreinest PA, Childs AC, Belmonte LS, LeGrand SN, Wu KJ, Luxon BA, Sinha M, Parker AS, et al: Secreted frizzled-related protein 1 loss contributes to tumor phenotype of clear cell renal cell carcinoma. Clin Cancer Res 13: 4740-4749, 2007.
23. Tun HW, Marlow LA, von Roemeling CA, Cooper SJ, Kreinest P, Wu K, Luxon BA, Sinha M, Anastasiadis PZ and Copland JA: Pathway signature and cellular differentiation in clear cell renal cell carcinoma. PLoS One 5: e10696, 2010.
24. Jones J, Otu H, Spentzos D, Kolia S, Inan M, Beecken WD, Fellbaum C, Gu X, Joseph P, Pantuck AJ, et al: Gene signatures of progression and metastasis in renal cell cancer. Clin Cancer Res 11: 5730-5739, 2005.
25. Brannon AR, Reddy A, Seiler M, Arreola A, Moore DT, Pruthi RS, Wallen EM, Nielsen ME, Liu H, Nathanson KL, et al: Molecular stratification of clear cell renal cell carcinoma by consensus clustering reveals distinct subtypes and survival patterns. Genes Cancer 1: 152-163, 2010.
26. Valletti A, Gigante M, Palumbo O, Carella M, Divella C, Sbisà E, Tullo A, Picardi E, D'Erchia AM, Battaglia M, et al: Genome-wide analysis of differentially expressed genes and splicing isoforms in clear cell renal cell carcinoma. PLoS One 8: e78452, 2013.
27. Wotschofsky Z, Gummlich L, Liep J, Stephan C, Kilic E, Jung K, Billaud JN and Meyer HA: Integrated microRNA and mRNA signature associated with the transition from the locally confined to the metastasized clear cell renal cell carcinoma exemplified by miR-146-5p. PLoS One 11: e0148746, 2016.
28. Gerlinger M, Horswell S, Larkin J, Rowan AJ, Salm MP, Varela I, Fisher R, McGranahan N, Matthews N, Santos CR, et al: Genomic architecture and evolution of clear cell renal cell carcinomas defined by multiregion sequencing. Nat Genet 46: 225-233, 2014.
29. von Roemeling CA, Radisky DC, Marlow LA, Cooper SJ, Grebe SK, Anastasiadis PZ, Tun HW and Copland JA: Neuronal pentraxin 2 supports clear cell renal cell carcinoma by activating the AMPA-selective glutamate receptor-4. Cancer Res 74: 4796-4810, 2014.
30. Ritchie ME, Phipson B, Wu D, Hu Y, Law CW, Shi W and Smyth GK: limma powers differential expression analyses for RNA-sequencing and microarray studies. Nucleic Acids Res 43: e47, 2015.
31. R Core Team: R: A language and environment for statistical computing. R Foundation for Statistical Computing, Vienna, Austria. ISBN 3-900051-07-0, 2012. http://www.R-project.org/.
32. Kolde R, Laur S, Adler P and Vilo J: Robust rank aggregation for gene list integration and meta-analysis. Bioinformatics 28: 573-580, 2012.
33. Huang da W, Sherman BT and Lempicki RA: Systematic and integrative analysis of large gene lists using DAVID bioinformatics resources. Nat Protoc 4: 44-57, 2009.
34. Huang da W, Sherman BT and Lempicki RA: Bioinformatics enrichment tools: Paths toward the comprehensive functional analysis of large gene lists. Nucleic Acids Res 37: 1-13, 2009.
35. Szklarczyk D, Morris JH, Cook H, Kuhn M, Wyder S, Simonovic M, Santos A, Doncheva NT, Roth A, Bork P, et al: The STRING database in 2017: Quality-controlled protein-protein association networks, made broadly accessible. Nucleic Acids Res 45: D362-D368, 2017.
36. Shannon P, Markiel A, Ozier O, Baliga NS, Wang JT, Ramage D, Amin N, Schwikowski B and Ideker T: Cytoscape: A software environment for integrated models of biomolecular interaction networks. Genome Res 13: 2498-2504, 2003.
37. Chin CH, Chen SH, Wu HH, Ho CW, Ko MT and Lin CY: cytoHubba: Identifying hub objects and sub-networks from complex interactome. BMC Syst Biol 8 (Suppl 4): S11, 2014.
38. Livak KJ and Schmittgen TD: Analysis of relative gene expression data using real-time quantitative PCR and the 2(-Delta Delta C(T)) method. Methods 25: 402-408, 2001.
39. Joeckel E, Haber T, Prawitt D, Junker K, Hampel C, Thüroff JW, Roos FC and Brenner W: High calcium concentration in bones promotes bone metastasis in renal cell carcinomas expressing calcium-sensing receptor. Mol Cancer 13: 42, 2014.
40. Rasti A, Abolhasani M, Zanjani LS, Asgari M, Mehrazma M and Madjd Z: Reduced expression of CXCR4, a novel renal cancer stem cell marker, is associated with high-grade renal cell carcinoma. J Cancer Res Clin Oncol 143: 95-104, 2017.
41. Zhang Y, Zhu X, Qiao X, Sun L, Xia T and Liu C: Clinical implications of HSC70 expression in clear cell renal cell carcinoma. Int J Med Sci 18: 239-244, 2021.
42. Luo Y, Shen D, Chen L, Wang G, Liu X, Qian K, Xiao Y, Wang X and Ju L: Identification of 9 key genes and small molecule drugs in clear cell renal cell carcinoma. Aging (Albany NY) 11: 6029-6052, 2019.
43. Du GW, Yan X, Chen Z, Zhang RJ, Tuoheti K, Bai XJ, Wu HH and Liu TZ: Identification of transforming growth factor beta induced (TGFBI) as an immune-related prognostic factor in clear cell renal cell carcinoma (ccRCC). Aging (Albany NY) 12: 8484-8505, 2020.
44. Cui T, Guo J and Sun Z: A computational prognostic model of lncRNA signature for clear cell renal cell carcinoma with genome instability. Expert Rev Mol Diagn 22: 213-222, 2022.
45. Yap NY, Ong TA, Pailoor J, Gobe G and Rajandram R: The significance of CD14 in clear cell renal cell carcinoma progression and survival prognosis. Biomarkers 28: 24-31, 2023.
46. Smith AN, Borthwick KJ and Karet FE: Molecular cloning and characterization of novel tissue-specific isoforms of the human vacuolar H(+)-ATPase C, G and d subunits, and their evaluation in autosomal recessive distal renal tubular acidosis. Gene 297: 169-177, 2002.
47. Nishisho T, Hata K, Nakanishi M, Morita Y, Sun-Wada GH, Wada Y, Yasui N and Yoneda T: The a3 isoform vacuolar type H⁺-ATPase promotes distant metastasis in the mouse B16 melanoma cells. Mol Cancer Res 9: 845-855, 2011.
48. Avnet S, Di Pompo G, Lemma S, Salerno M, Perut F, Bonuccelli G, Granchi D, Zini N and Baldini N: V-ATPase is a candidate therapeutic target for Ewing sarcoma. Biochim Biophys Acta 1832: 1105-1016, 2013.
49. Xu J, Xie R, Liu X, Wen G, Jin H, Yu Z, Jiang Y, Zhao Z, Yang Y, Ji B, et al: Expression and functional role of vacuolar H(+)-ATPase in human hepatocellular carcinoma. Carcinogenesis 33: 2432-2440, 2012.
50. Lu Q, Lu S, Huang L, Wang T, Wan Y, Zhou CX, Zhang C, Zhang Z and Li X: The expression of V-ATPase is associated with drug resistance and pathology of non-small-cell lung cancer. Diagn Pathol 8: 145, 2013.
51. Kulshrestha A, Katara GK, Ibrahim S, Pamarthy S, Jaiswal MK, Gilman Sachs A and Beaman KD: Vacuolar ATPase 'a2' isoform exhibits distinct cell surface accumulation and modulates matrix metalloproteinase activity in ovarian cancer. Oncotarget 6: 3797-3810, 2015.
52. Huang L, Lu Q, Han Y, Li Z, Zhang Z and Li X: ABCG2/V-ATPase was associated with the drug resistance and tumor metastasis of esophageal squamous cancer cells. Diagn Pathol 7: 180, 2012.
53. Michel V, Licon-Munoz Y, Trujillo K, Bisoffi M and Parra KJ: Inhibitors of vacuolar ATPase proton pumps inhibit human prostate cancer cell invasion and prostate-specific antigen expression and secretion. Int J Cancer 132: E1-E10, 2013.

54. Chung C, Mader CC, Schmitz JC, Atladottir J, Fitchev P, Cornwell ML, Koleske AJ, Crawford SE and Gorelick F: The vacuolar-ATPase modulates matrix metalloproteinase isoforms in human pancreatic cancer. Lab Invest 91: 732-743, 2011.
55. Cotter K, Capecci J, Sennoune S, Huss M, Maier M, Martinez-Zaguilan R and Forgac M: Activity of plasma membrane V-ATPases is critical for the invasion of MDA-MB231 breast cancer cells. J Biol Chem 290: 3680-3692, 2015.
56. Forgac M: Vacuolar ATPases: Rotary proton pumps in physiology and pathophysiology. Nat Rev Mol Cell Biol 8: 917-929, 2007.
57. McGuire C, Cotter K, Stransky L and Forgac M: Regulation of V-ATPase assembly and function of V-ATPases in tumor cell invasiveness. Biochim Biophys Acta 1857: 1213-1218, 2016.
58. Schneider LS, von Schwarzenberg K, Lehr T, Ulrich M, Kubisch-Dohmen R, Liebl J, Trauner D, Menche D and Vollmar AM: Vacuolar-ATPase inhibition blocks iron metabolism to mediate therapeutic effects in breast cancer. Cancer Res 75: 2863-2874, 2015.
59. Schempp CM, von Schwarzenberg K, Schreiner L, Kubisch R, Müller R, Wagner E and Vollmar AM: V-ATPase inhibition regulates anoikis resistance and metastasis of cancer cells. Mol Cancer Ther 13: 926-937, 2014.
60. Wiedmann RM, von Schwarzenberg K, Palamidessi A, Schreiner L, Kubisch R, Liebl J, Schempp C, Trauner D, Vereb G, Zahler S, *et al*: The V-ATPase-inhibitor archazolid abrogates tumor metastasis via inhibition of endocytic activation of the Rho-GTPase Rac1. Cancer Res 72: 5976-5987, 2012.
61. Kubisch R, Fröhlich T, Arnold GJ, Schreiner L, von Schwarzenberg K, Roidl A, Vollmar AM and Wagner E: V-ATPase inhibition by archazolid leads to lysosomal dysfunction resulting in impaired cathepsin B activation in vivo. Int J Cancer 134: 2478-2488, 2014.
62. Capecci J and Forgac M: The function of vacuolar ATPase (V-ATPase) a subunit isoforms in invasiveness of MCF10a and MCF10CA1a human breast cancer cells. J Biol Chem 288: 32731-32741, 2013.